

Simulation of Stresses Induced by Heat and Mass Transfer in Drying Process of Clay-like Material

M. Heydari^{1,*}, K. Khalili², S. Y. Ahmadi-Brooghani³

¹Ph.D. Student, Department of Mechanical Engineering, University of Birjand, Birjand, Iran

²Prof., Department of Mechanical Engineering, University of Birjand, Birjand, Iran

³Assoc. Prof., Department of Mechanical Engineering, University of Birjand, Birjand, Iran

Received: 3 July. 2017, Accepted: 7 Aug. 2017

Abstract

Drying represents one of the oldest unit operations employed in industrial processes. Drying is viewed as a process of simultaneous heat and mass transfer. Porous Clay-like material undergoes stresses due to non-uniform distribution of temperature and moisture induced by heat and mass transfer respectively. The aim of this work is to simulate the stresses induced by heat and mass transfer during drying. A mathematical model to simulate the convective drying of a porous material like clay has been developed. The problem investigated involves highly coupled equations considering heat, mass, and mechanical aspects. The particularity of the model is that it takes into account the strong coupling between mass transport, heat transport and mechanical behavior of the material. The variables of coupling are the solid deformation, moisture content and temperature of porous medium. A numerical solution is sought to foresee the variation of moisture content, temperature, shrinkage, heat transfer induced stresses and mass transfer induced stresses during drying. The solution developed as a model is capable of predicting the quality of the product through a failure criterion. The model is validated through the comparison of simulated and experimental data. Simulation results show that the heat transfer induced stresses are 125E3 times higher than the mass transfer induced stresses and can be neglected in modeling of drying process.

Keywords:

Convective drying, Modeling, Drying Stresses, Heat Transfer, Mass Transfer.

* Corresponding Author.

Email Address; m.heydari@birjand.ac.ir

1. Introduction

Industrial drying is an essential process in manufacturing of many products as diverse as from food products to clay/ceramic products. Drying is also an energy intensive operation that easily accounts for up to 15% of all industrial energy usage [1]. The process usually influences the quality of the resulting product. Severe conditions and long drying time can significantly decrease the quality of dried materials; e.g., by change of color [2], permanent deformation (shrinkage) and material damage [3]

Modeling of kinetics and drying processes should be determined to effectively control the drying process. It is important to choose suitable conditions of drying for a specific product. Modeling of drying process is inherently a coupled and complex problem. Several particular problems, which are generally highly coupled, are present in the drying process: Drying kinetics change, deformation, and product structure change. The change in moisture content affects the thermal, moisture, and mechanical properties of the material [4] and shrink/swell the solid matrix during drying. Generally, the drying process modeling is composed of the equations of mass, heat, and momentum conservation forming a system of partial differential equations.

Moisture transfer in porous materials can be accomplished by several transport mechanisms, such as moisture diffusion due to concentration gradients, Thermo diffusion, Knudsen diffusion, capillary flow, evaporation and condensation [5]. Although all these transport mechanisms have a strong physical basis, moisture diffusion, is the most important mass transport mechanism [6] which is expressed by Fick's equation.

Taking all of the transport mechanisms in the drying process into consideration makes a very complex problem rendering the solution infeasible. Furthermore, most drying conditions are such that only one or two of the mentioned mechanisms are important. The most common approach in engineering applications to overcome the problem and to take into account the relevant mechanisms is to lump all effects of the transport mechanisms onto the diffusion coefficient in Fick's law. Thus, the diffusion coefficient becomes an effective coefficient. In this study the diffusive model based on the phenomenon of diffusion described by Fick's law was used for the description of moisture movement. Fick's law with an effective diffusion coefficient has already been used successfully by many authors in mathematical model of drying process [7-9].

The material properties of the product may change during drying. The added complexity of identification and considering of the material properties changes obliged a wide range of study to use constant parameters

in the models dealing with drying [10-12]. Indeed, most products cannot completely fit into simplified model and need complex model which takes into account the variation of material properties with moisture content and temperature. The current study takes into account the material properties variations during drying.

Drying of many materials is accompanied by shrinkage. If drying is performed sufficiently slow, the shrinkage would be uniform and drying induced stresses do not occur, but for economical reasons the industrial drying process is usually performed fast in such a way that the non-uniform shrinkage is usually arises. Differential shrinkage from the surface to the core is responsible for high tensile stresses. Drying-induced stresses are expressed as the sum of the heat transfer induced stresses (thermal stresses) and moisture transfer induced stresses (moisture stresses). Numerical investigation of the drying stresses was started in 1970s [13]. A number of studies can be found in the literature dealing with the moisture stresses induced during drying.

Chemkhi et al described the mass, heat and momentum conservation equations separately for liquid and solid phase and by using effective stress concept derived the moisture stresses [14]. The influence of rheological aspect assigned to a deformable and saturated porous medium on the moisture stresses was studied by Khalfaoui et al [15]. Couture et al simulated the moisture stresses for liquid phase during drying by assuming ideal shrinkage [16]. Most authors suggest comparing simulated tensile stresses with a failure criterion in order to obtain the range of drying conditions under which the cracking of materials is avoided [17-19]. Pourcel et al investigated crack initiation time during drying and stated that it depends on drying rate [20]. Some works have been published concerning the experimental measurement of thermal field of clay during drying [21, 22].

Surveying the literature reveals that the thermal stresses have not been studied. The novelty of the current study is investigation the thermal stresses in drying process. Having considered the heat, mass, and mechanical aspects of drying the drying kinetics of 3D moist object was modeled and simulated. The variables of coupling are the solid deformation, moisture content and temperature of porous medium.

2. Convective drying Periods of clay

Four periods may distinguished in convective drying of clay as follow: preheating period, constant drying rate period (CDRP), falling drying rate period (FDRP) and transition period (Fig. 1). In the preheating period the material with initial temperature (T_0) starts to be heat

up/down to the wet bulb temperature (T_w) (F-J or G-J) and consequently the drying rate will also start to drop/rise (A-C or B-C), respectively [23]. The CDRP begins at time t_w in Fig. 1. At this point; the temperature of the material is equal to the wet bulb temperature (J) and remains constant (J-K). The CDRP is governed fully by the rates of external heat and mass transfer since a film of free water is always available at the evaporating surface. The moisture migrates from the inside of the porous material to the surface by diffusion of moisture [24]. The drying rate remains constant as long as the moisture transport rate from the interior of the material to the exchange surface can withstand the evaporation rate from the exchange surface (C-D). The moisture content at the end of the CDRP is called the critical moisture content (w_{cr}) point (D). At the end of the CDRP (D), the evaporation rate starts to decrease because of the disconnection of the liquid meniscus from the surface and this decreasing trend continues until all the liquid meniscuses are disconnected. This period is termed as the transition period (D-O or K-O). Detachment of the last liquid meniscus from the surface marks the onset of FDRP (O). The internal moisture transport rate specifies the drying rate of the FDRP. During the transition period and the FDRP the temperature of material surpasses the wet bulb temperature and grows up to the drying air temperature (K-L). Finally, the drying process stops when the equilibrium moisture content (w_{eq}) reaches.

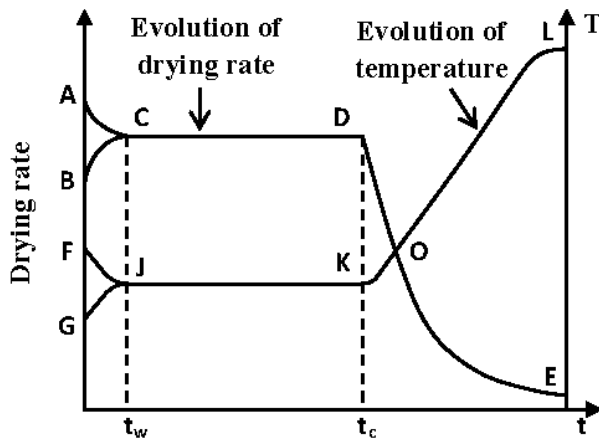


Fig. 1 Dependence of moisture content and temperature on drying time of clay

Several types of strains are expected to exist when drying the clay including; moisture, thermal, mechanical, creep and mechano-sorptive strains. The moisture and thermal

Usually the maximum moisture and temperature non-uniformity occurs at the end of the CDRP [21] hence material cracking is most possible to happen at this stage of drying [6, 25]. This is the reason why large bodies of study are devoted to the CDRP [26-28].

3. Shrinkage considerations

Shrinkage or Solid displacement is one of the most important coupling parameter in the system of drying equation. Shrinkage has strong effect on drying behavior of highly shrinkable porous media such as clay-like material.

During drying process, non-uniform shrinkage creates stresses which may causes cracking and directly influence the quality of dried products or even make them useless.

Another important effect of the shrinkage on drying behavior is the reduction of drying surface; resulting decreased drying rate. Drying rate has direct effect on the drying time and intensity of the non-uniform distribution of the moisture and temperature, and consequently on the drying induced stresses magnitudes. Fig. 2 presents the effect of the shrinkage consideration on the drying curve [21]. It is observed that ignoring the shrinkage during the constant drying rate period, overestimates the drying rate but the difference between the two states (ignoring and considering the shrinkage) disappears as soon as the falling period of drying starts.

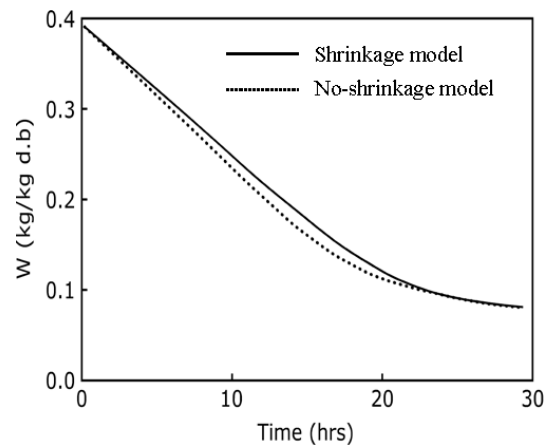


Fig. 2 Shrinkage effect on drying behavior[21]

strain are assumed to be proportional to the moisture content and temperature change, respectively and are independent of the state of stress [11]. Mechanical strains

include elastic or plastics strains that are formed immediately after application of mechanical loading (drying induced stresses). Creep is the time-dependent increment of total deformation due to imposed stress history which is an irreversible strain. Some authors introduce an extra mechano-sorptive/desorptive strain that results from the interaction between stress and moisture content change [29].

To calculate the deformations by drying induced stresses, the momentum balance equations in addition to the diffusion equations must be solved leading to a series of differential equations. Many studies considered shrinkage of the material to be equal to the volume of the evaporated water (ideal shrinkage) during the two first phases of drying and neglected mechanical strains [9, 16, 25, 30, 31].

Many researcher have considered shrinkage during the drying process in their studies, however some ignored it completely [32]. But it is necessary to incorporate the shrinkage into the drying model especially when dealing with building materials like wood and ceramics, where shrinkage is a key aspect of the dehydration phenomena [33]. In the current study the thermal strains, moisture strains which mostly is the largest strain component in drying and the mechanical elastic and plastic strains, which are activated by the drying-induced stresses, are taken into account. The plastic strains arise when the state of stress reaches the yield condition. Also the mean moisture content evolution of material, with and without considering the shrinkage effect has been illustrated presented in the rest of the text.

4. Mathematical modeling

One of the important parts of modeling is providing an appropriate mathematical model. In this section, the mathematical model describing the drying process of saturated and shrinking media is presented. The particularity of the model is that it takes into account the strong coupling between mass transport, heat transfer and mechanical behavior of the material. The model takes into account the shrinkage via the mechanical behavior of the material that is assumed to be elastic. The following assumptions have been made to solve the problem.

- Clay is a homogeneous and isotropic porous material.
- Local thermal equilibrium is assumed.
- The mechanical behavior of the medium is purely elastic.
- Gaseous phase and gravitational effect are neglected.

With regard to the assumptions, the system of equations describing heat and mass transfer takes the following form:

$$\frac{\partial w}{\partial t} = \nabla \cdot (D_{eff} \nabla w) \quad (1)$$

$$\rho C_p \frac{\partial T}{\partial t} = \nabla \cdot (k \nabla T) \quad (2)$$

Where D_{eff} is effective diffusion coefficient. The eq. 1

and 2 are coupled through D_{eff} , ρ and C_p , parameters.

The balance of momentum in our considerations is limited to:

$$\nabla \cdot \sigma = 0 \quad (3)$$

If we consider the assumption of small deformation, the volume change depends on temperature and moisture variations. Therefore, the moisture and thermal strains (respectively ε^H and ε^T) are subtracted from the total strain to get the mechanical strain:

$$\varepsilon_M = \varepsilon - \varepsilon_w - \varepsilon_T, \varepsilon_T = \alpha(T - T_0), \varepsilon_w = \beta(w - w_0) \quad (4)$$

Here α is the thermal expansion and β is the moisture expansion coefficient. In the case of elastic behavior, the constitutive equation for strain–stress is given by [11]:

$$\sigma = \lambda \text{tr}(\varepsilon) \mathbf{I} + 2\mu \varepsilon - 3K\beta(w - w_0) \mathbf{I} - 3K\alpha(T - T_0) \mathbf{I} \quad (5)$$

Where K is the bulk modulus, λ and μ are the Lamé constants related to the Young modulus E and the Poisson ratio ν as:

$$\lambda = \frac{E\nu}{(1-2\nu)(1+\nu)}, \mu = \frac{E}{2(1+\nu)}, K = \frac{E}{3(1-2\nu)} \quad (6)$$

5. Initial and boundary conditions

Initially, the temperature and moisture content are uniform in the porous medium, that is:

$$t = 0, \quad T = T_0, \quad w = w_0 \quad (7)$$

The values of the parameters used in the simulations are given in Table 1. The heat flux and the mass flux at the exchange surface are expressed as:

$$-D_{eff} \nabla w = F_m \quad (8)$$

$$-k \nabla T = h(T_s - T_{inf}) - h_v F_m \quad (9)$$

Where F_m is the rate of evaporation at the surface, h_v is the latent heat of evaporation, h and k are convection and conduction heat transfer coefficient respectively. At the exchange surface, there are no external forces and the deformation is due to the water evaporation:

$$\sigma.n = 0$$

6. Simulation

The finite element method has been used to solve this strongly coupled and nonlinear system of equations. The Arbitrary Lagrange-Eulerian formulation was used. This is actually a combo system of Lagrangian and Eulerian systems, combining the two systems to solve the problem with moving boundaries. This allows consideration of a

drying process of a shrinking body, as is the case in the current study. The constant and variable parameters employed in simulation are presented in Table 1 and Table 2, respectively

Simulation is carried out in a cubic sample having dimension of 7cm*7cm*5cm with a constant time step (dt =50s). Fig. 3 presents the schematic illustrations of the problem domain. The simulated domain is discretized by 11342 tetrahedral elements regularly spaced at beginning.

Table 1: Employed constant parameters in modeling

Parameter	value
Initial moisture content	$w_0 = 0.33$
Critical moisture content	$w_{cr} = w_{sh} = 0.12$
Equilibrium moisture content	$w_{eq} \approx 0.01$
Initial sample temperature	$T_0 = 26^\circ C$
Intrinsic clay density [25]	$\rho_s^s = 2600 (kg / m^3)$
Intrinsic water density [5]	$\rho_l^l = 1000 (kg / m^3)$
Solid thermal conductivity [14]	$k_s = 1 (W / mK)$
Liquid thermal conductivity [34]	$k_l = 0.597 (W / mK)$
Solid specific heat [14]	$C_{ps} = 2000 (J / kg)$
Liquid specific heat [5]	$C_{pl} = 4220 (J / kg)$
Heat expansion coef [35]	$\alpha = 3 \times 10^{-8} (1 / K)$
mass expansion coef [36]	$\beta = 0.3$
Poisson's ratio [14]	$\nu = 0.4$

Table 2: Employed variable parameters in modeling

Parameter	Expression
Specific heat [37]	$C_p = \frac{wC_{pl} + C_{ps}}{w + 1} (J / kg)$
Density [37]	$\rho = \frac{m_0(1 + w)}{V(1 + w_0)} (kg / m^3)$
Young's modulus [14]	$E = 0.96 \exp\left(\frac{1}{0.061 + 1.735w^{4.919}}\right) (Pa)$
Effective diffusion coefficient [34]	$D_{eff} = 5.61e^{-9} (7.5 + \exp\left(\frac{44w}{1.6 + w}\right) \times \exp\left(-\frac{510}{T}\right)) (m^2 / s)$
Evaporation rate [15, 38]	$F_m = \begin{cases} \dot{m} & \text{for } w > w_{cr} \\ \dot{m} * \frac{w - w_{eq}}{w_{cr} - w_{eq}} & \text{for } w < w_{cr} \end{cases}$ $\dot{m} = 13 * 10^{-3} * (C_{surf} - C_{inf}) (kg / m^2 s)$ $C_{inf} = \frac{0.622RH.P_{vs.inf}}{P_{atm} - RH.P_{vs.inf}}$ $C_{surf} = \frac{0.622a_w.P_{vs.surf}}{P_{atm} - a_w.P_{vs.surf}}$ $P_{vs.inf} = \exp\left(23.3265 - \frac{3802.7}{T_{inf}} - \left(\frac{472.68}{T_{inf}}\right)^2\right)$ $P_{vs.surf} = \exp\left(23.3265 - \frac{3802.7}{T_{surf}} - \left(\frac{472.68}{T_{surf}}\right)^2\right)$

7. Material and experimental procedure

7.1. Material

All the clay-like material used for the experiment were extracted from clay deposit sites in Birjand-Iran. Chemical analysis (Table 3) and Atterberg limits (Table

4) of the studied clay are determined in Soil Mechanics & Technical Laboratory of Mashhad-Iran.

Table 3: Chemical analysis of the Clay

Element	Percent
Si	59.5
Ca	7.83
Mg	4.20
Fe	4.50
Al	7.80
Ti, Mn	<1
L.O.I	9.80

Table 4: Atterberg limits of the Clay

Atterberg Limits	Moisture content
Liquid limit	26%
Plastic limit	19%
Shrinkage limit (w_{sh})	12%

7.2. Experimental equipment set-up

A laboratory chamber dryer was used for experimental study. A schematic of experimental setup is shown in Fig 4. The sample is located on a grid plate (holder) at the center of the dryer chamber. The holder is placed on the A&D GF3000 digital balance with 0.01 gram resolution. The air-stream generated by the blower passes through a controlled heating zone, enters the dryer chamber. In order to provide uniform drying condition for all of the surfaces of sample, the air-stream enters both from the top and bottom and exits from the four

vents located at the center of the all lateral sides of the dryer chamber.

The temperature and relative humidity of the chamber are measured and logged in computer during drying by using a humidity temperature sensor (SHT25) connected to the national instrument usb-6009 data acquisition card. The measurement accuracy of the SHT25, is 0.2°C and 1.8% for the temperature and the relative humidity, respectively. The temperature and humidity are kept at set levels using feedback control. Also the geometry variations of the sample were captured by using a digital camera. The chamber dryer equipped with two Halogen lamps positioned at fixed location illuminating the scene evenly.

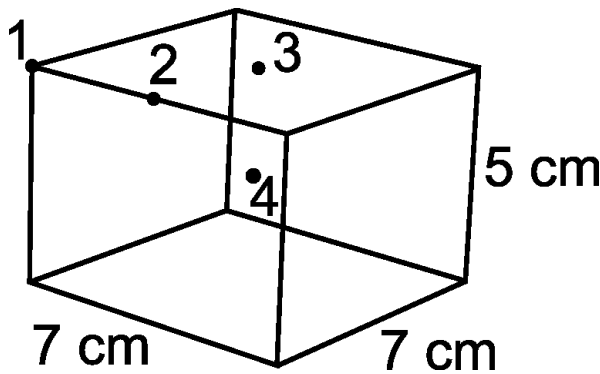


Fig. 3 Schematic view of the sample geometry

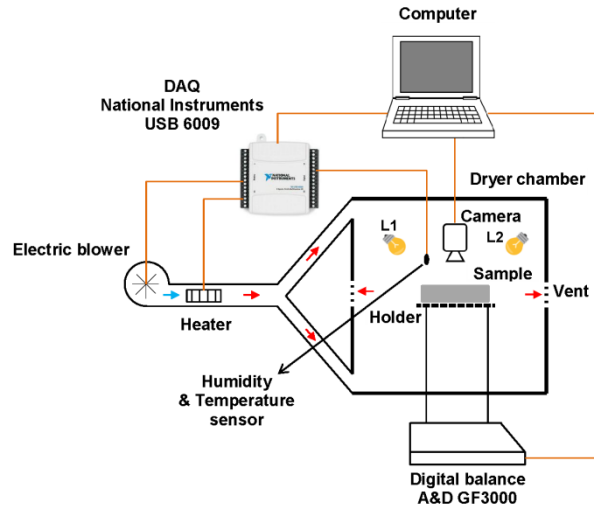


Fig. 4: Schematic of experimental setup

7.3. Model Application to Clay Drying

The model developed was validated by comparing the model outputs (simulation results) with experimental results. The experiment was carried out in the laboratory chamber dryer. A cubic sample of clay material, with an approximate dimension of $7 \times 7 \times 5 \text{ cm}$ was placed on the holder and the airstream circulated over samples surface. The clay was mixed with water to make a workable paste with approximately 33% (dry basis). Then the clay paste was stored in an airtight container at room temperature (26°C) for 48 hour to make sure that the water content is uniform throughout the material providing a homogenized sample. The Cubic sample was dried at 100°C with a relative humidity of 10%.

The drying process was controlled by a PC provided with the software and data acquisition card. During the experimental run the following parameters were controlled and recorded: drying time, air temperature, air relative humidity, geometry variations and mass of the sample. The mass evolution of the sample was logged to computer every 10 seconds by the precision digital balance. During the experimental run, snapshots of the surface shrinkage for the top surface and one of side surfaces were taken every 15 minutes. Volumetric shrinkage of the sample was calculated using image processing techniques (Fig 5).

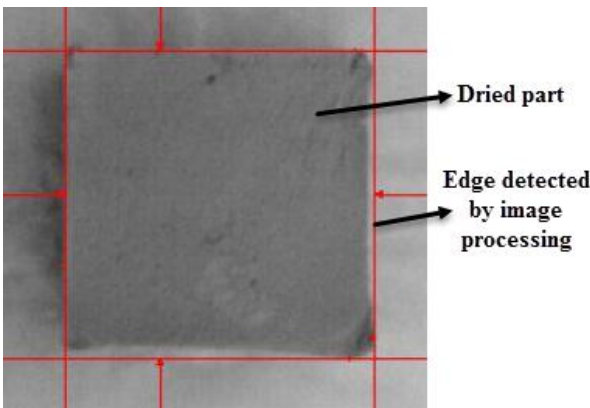


Fig. 5: Edge detection by image processing during the experiment run

According to the Atterberg limits in drying process, clay shrinks only when the moisture content is above shrinkage limit (w_{sh}). In the current study the shrinkage limit and critical moisture content are assumed to be the same; $w_{sh} = w_{cr} = 0.12$. This assumption has been made in other works dealing with clay material drying [40, 41]. Fig. 8 shows the comparison between the experimental results and the simulated values of the volumetric strain

Fig. 6 shows the comparison between the experimental results and the simulated values of the mean moisture contents evolution for clay sample. The sample is dried after about 12 hours. The water vapor condenses onto the sample's surfaces at the beginning of drying, since for the chosen air conditions the dew point corresponds to 46°C , which is greater than the sample's initial temperature of 26°C . Consequently, the moisture content increases and a swelling of the medium occurs and continues until the dew temperature is reached when condensation stops. The points A, B, C and D in Fig. 6 to Fig. 10 corresponds to the end of the preheating period, the end of the CDRP, the end of transition period and the end of FDRP, respectively.

Fig.7 illustrates the evolution of the mean temperature inside the product. The temperature exhibits the classical evolution that occurs during convective drying. The three phases are clearly present: Phase 1 is the preheating period where the material is heated until its temperature reaches the wet bulb temperature (52°C); Phase 2 is the CDRP, during which the diffusion of water from inside of the sample keeps up with the evaporation rate. The whole heat supplied by the air is consumed by the water evaporation at the surface and the temperature keeps constant [39]. Phase 3, is the transition period and the FDRP, during which the temperature begins to grow with the time and trends to the drying air temperature.

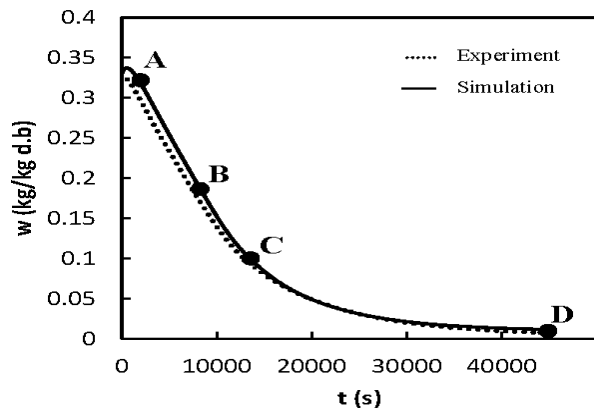


Fig. 6: Average moisture content changes

for clay sample. As seen from Fig. 8 the clay sample shrinks mainly in the preheating and the CDRP, and during the transition period and the FDRP, the sample volume is approximately constant. The volumetric strain of the sample is about 17%.

The evaporation rate in the CDRP is supplied by the capillary flow from the material depth to the evaporation surface in porous clay-like material. During this period,

evaporation occurs at the surface. At the critical moisture content which is the end of the CDRP, evaporation rate starts to decrease because of the disconnection of the liquid meniscus from the surface and this decreasing trend continues until all the liquid menisci are disconnected. This period was termed as the transition period. Detachment of the last liquid meniscus from the surface marks the onset of the FDRP and changing the vaporization plane to a level below the surface [42].

The experimental results and the simulated values of the drying rate for clay sample are compared in Fig. 9. In the preheating period because of increase in sample temperature, drying rate increase until it reaches the wet bulb temperature; (point A). The CDRP begins from point A and drying rate remains constant. Moisture evaporation at exchange surface occurs with higher rates and values at edges. As soon as the first point moisture content of edge's point arrive at the shrinkage limits the transition period begins (point B) and because of the disconnection of the liquid meniscus from the surface the evaporation rate starts to decrease. At point C which is almost the inflection point, all liquid menisci have been disconnected and FDRP begins. Following disruption of hydraulic continuity between the sample depth and exchange surface liquid menisci recede into the porous medium and form a vaporization plane from which water vapor diffuses through the overlying dry layer to the exchange surface and then to the atmosphere [43].

Fig. 10 shows the comparison between the experimental results and the simulated values of the density for clay sample. It is important to note that the

density increases at the beginning of drying, reaches a maximum at the time of 11000s which is almost the end of CDRP (point B) and then decreases. This evolution is the consequence of superposition of two phenomena: mass reduction and volume reduction. In preheating period and CDRP volume reduction is almost equal to the mass reduction (moisture removed by evaporation) from the sample (ideal shrinkage) [16]. Intrinsic clay density is more than water intrinsic density hence; the density increase until the end of CDRP. For moisture content below the critical limit the movement of the clay particles becomes more difficult and gradually the volume reduction stops. Therefore the effect of mass reduction dominates a decrease in the density. Similar results are reported in other works [41].

Fig. 11 shows the captured image of the sample surface during drying. Fig. 11a corresponds to the time that the moisture content at edge's point is just at the shrinkage limit and the CDRP has almost been ended. Fig. 11a corresponds to the point B in Fig. 6 to Fig. 10. Fig. 11b shows the captured image of sample surface when it is in the transition period. During this period some of the liquid menisci are disconnected. The domain of not disconnected liquid menisci is approximately separated from other with a bound. Fig. 11c shows the image taken at the end of transition period and the beginning of the FDRP when all the liquid menisci are disconnected and almost the sample stops to shrink. Fig. 11c corresponds to the point C Fig. 6 to Fig. 10.

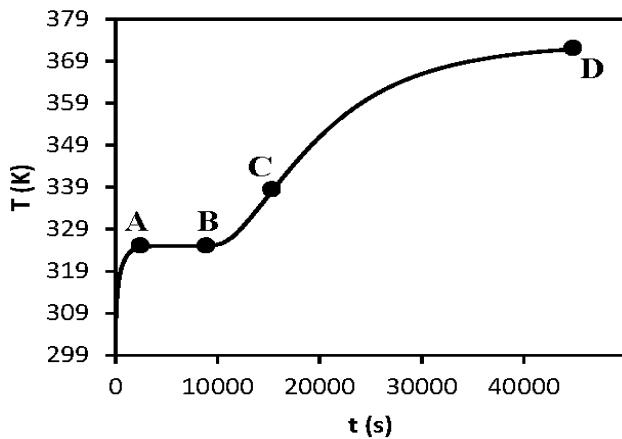


Fig. 7: Average temperature changes

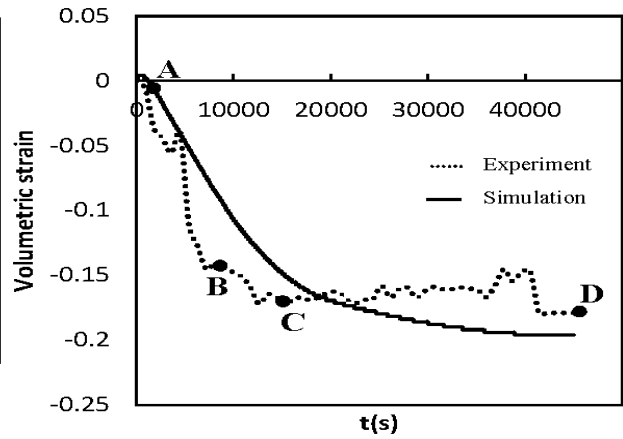


Fig. 8: Volumetric strain changes

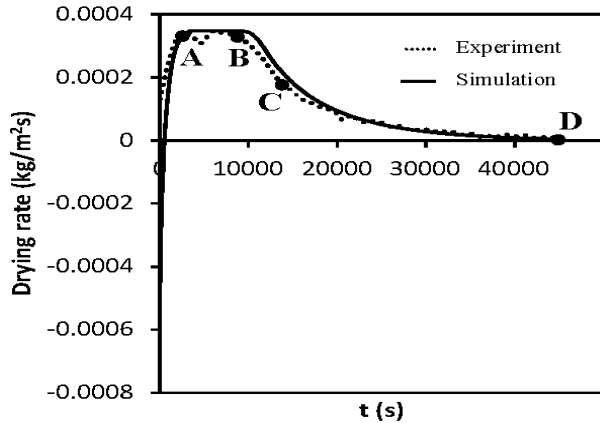


Fig. 9: Drying rate changes

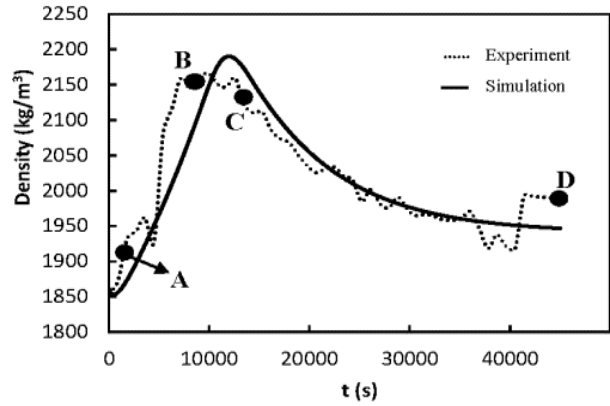


Fig. 10: Clay density changes with time

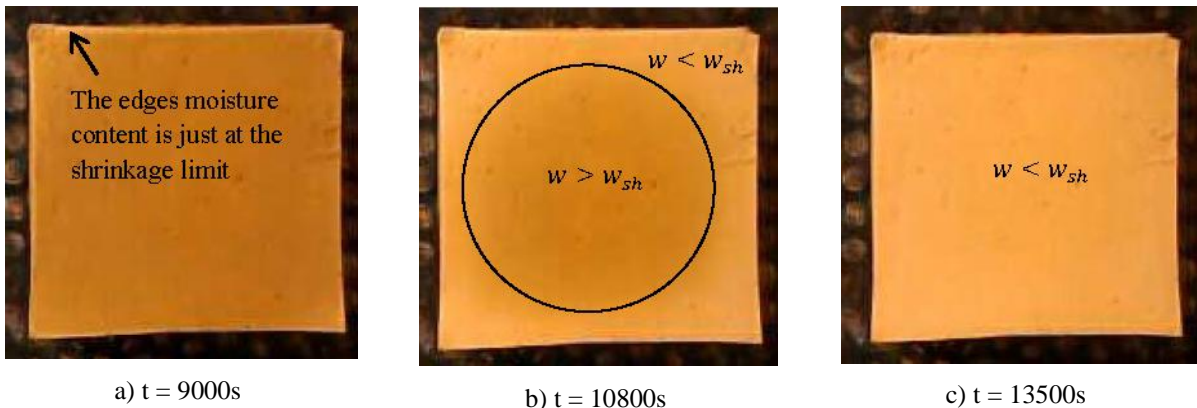


Fig. 11 the evolution of clay drying

To ensure that the results of simulation are not affected by changing the size of the elements; mesh convergence analysis has been done. The effect of element number on the moisture content evolution curve which is critical variable in simulation of drying kinetic was investigated. As seen in Fig. 12 the moisture content evolution curve regarding to discretization with 11342 and 22680 elements have good coherence but the moisture content evolution curve regarding to discretization with 3406 elements slightly differs. Increasing the number of elements increases the run time, on the other hand the moisture content evolution curve affects the drying induced stress heavily therefore 11342 numbers of elements was used in this study.

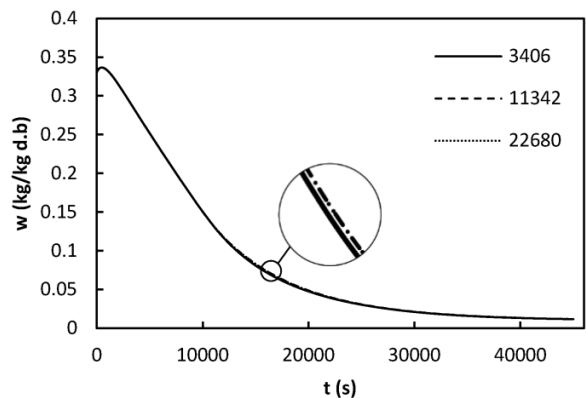


Fig. 12 the effect of element number on the moisture content evolution curve

The experimental and numerical results for drying kinetic, volumetric strain, drying rate and density show a good agreement between to each other. The mean absolute percent error (MAPE) of moisture content, volumetric strain, drying rate and density evolution curve is 8.7%, 2.26%, 1.61% and 0.17%, respectively. The MAPE values obtained shows less value compared to other studies [6, 7, 11, 15]. It shows that the developed mathematical model is accurate for overall drying process. Therefore the simulation can be considered as useful tool to predict the stresses induced by drying and the quality of dried product.

8. Heat and mass transfer induced stresses

The moisture and temperature is uniform at the start of drying process. Evaporation/condensation of moisture from/onto the sample surface causes non uniform distribution of the moisture content and temperature. Fig. 12 shows the evolution of moisture content in four point of clay sample presented in Fig. 3. The moisture content decreases in the time that is the consequence of evaporation. The moisture content decreases in points 1, 2, 3 and 4 respectively. The gradient of the moisture content is always directed from the outside to inside of the material. It became maximum approximately at the end of CDRP and then it develops gradually to flatten at the end of drying when the points reach the equilibrium moisture content. The temperature distribution of the sample shows in Fig. 13. Temperature increases rapidly throughout the material in the beginning of the experiment and a temperature gradient develops in the material.

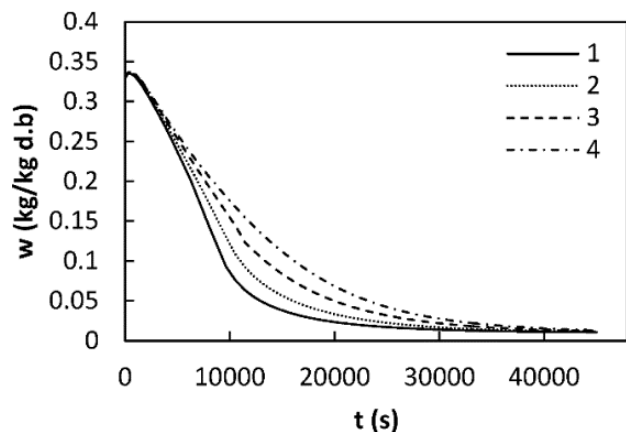


Fig. 13 Mean moisture evolution of the sample

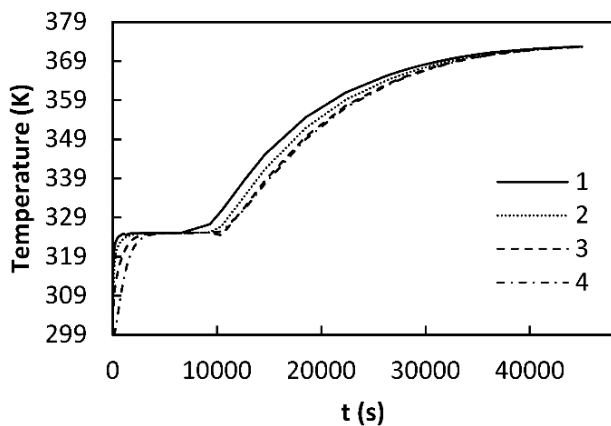


Fig. 14 Temperature evolution of the sample

The clay sample shrinks during drying which is the result of superposition of two phenomena: moisture content and temperature change. The volume strain induced by moisture content and temperature changes is shown in Fig. 14 and Fig. 15, respectively. The volume strain induced by moisture content changes is negative and cause the sample shrinkage but the volume strain induced by temperature content changes is positive and cause the sample expansion. The moisture strain is so greater than the temperature strain. The stress pattern in dried materials is due to non-uniform shrinkage induced by moisture content and temperature change. Fig. 16 shows the evaluation of Mises stress as a result of non-uniform shrinkage induced by moisture content changes and Fig. 17 shows the evaluation of Mises stress as a result of non-uniform expansion induced by temperature changes. The maximum of moisture induced stresses is about 250000 Pa and the maximum of temperature induced stresses is about 2 Pa. The temperature changes induced stresses are very small in comparison with the moisture changes induced stresses. Thus; the temperature changes induced stresses and their effects on drying kinetic can be neglected in drying process modeling. Both of maximum moisture stress and maximum temperature stress occur at the same point 2 located at the middle of the edge. Therefore this point is the most probable candidate point for crack initiation. It is important to note that heat transfer aspect of drying process has strong influence on the mass transfer and mechanical aspects of drying process and cannot be neglected in modeling.

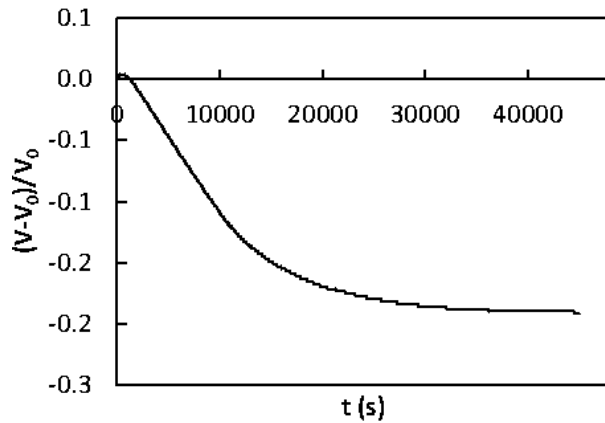


Fig. 15 Volume strain induced by moisture transfer

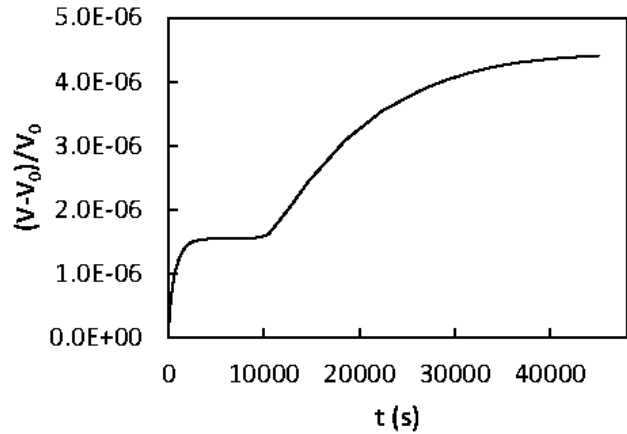


Fig. 16 Volume strain induced by heat transfer

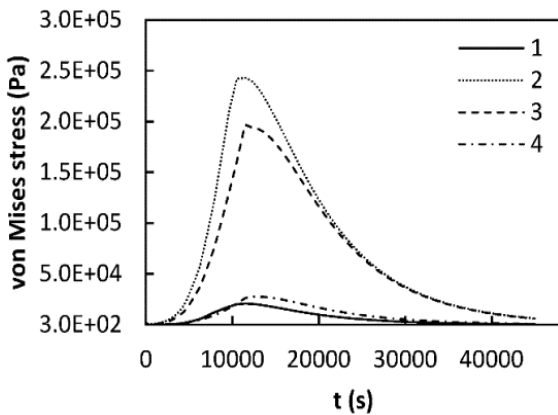


Fig. 17 Von mises stress evolution induced by moisture content changes

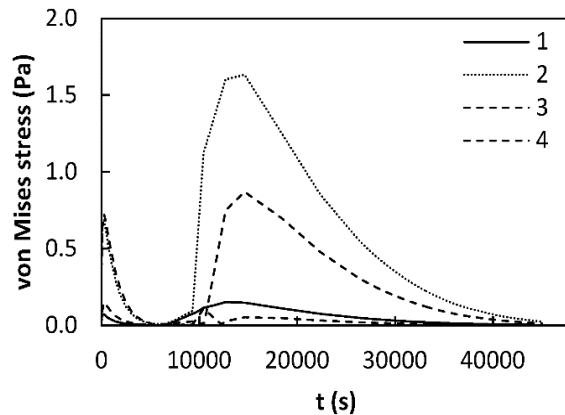


Fig. 18 Von mises stress evolution induced by temperature changes

9. Prediction of sample cracking

The quality of dried sample can be predicted by employing a failure criterion. The Von Mises yield criterion states that in order to prevent cracking the following condition has to be satisfied [17]:

$$\begin{aligned} & \text{yield stress} && (10) \\ & - \text{Von Mises stress} > 0 \end{aligned}$$

The yield stress depends on the moisture content and limit of the elastic behavior of the material when submitted to a uniaxial tension. For Clay, yield stress has been determined experimentally by Ketelaars [21]. Fig. 18 shows the comparison between maximum Mises stress induced by drying which belong to point 2 and

yield stress. It can be seen drying condition cannot lead to cracking since maximum Mises stress induced by drying is smaller than yield stress during drying. Fig. 19 shows the dried sample. The sample as was predicted by the model is free of any cracking.

10. Conclusions

A fully coupled model of drying process was developed to predict the stress–strain and clay–water characteristics response. The model was solved numerically to predict drying kinetic. The experimental results for drying kinetic, volumetric strain, drying rate and density show a good agreement with numerical results, validating the mathematical model of the drying process. Also the failure prediction of the dried sample reveals that simulation can be considered as a practical tool to predict

severe defects namely the cracking. Volume strain induced by moisture content and temperature changes were simulated. The evolution curves of strain were quite different. The volume strain induced by moisture content causing shrinkage is negative while the volume strain induced by temperature causing sample expansion is positive. The analysis of drying induced stresses shows that, the non-uniform heat expansion induced stresses are 125E3 times higher than non-uniform moisture

shrinkage induced stresses, thus; the non-uniform heat expansion induced stresses and the associated effects on drying kinetic can be neglected in modeling of drying process. It is important to note that heat transfer aspect of drying process has strong influence on the mass transfer and mechanical aspects of drying process and cannot be neglected in modeling.

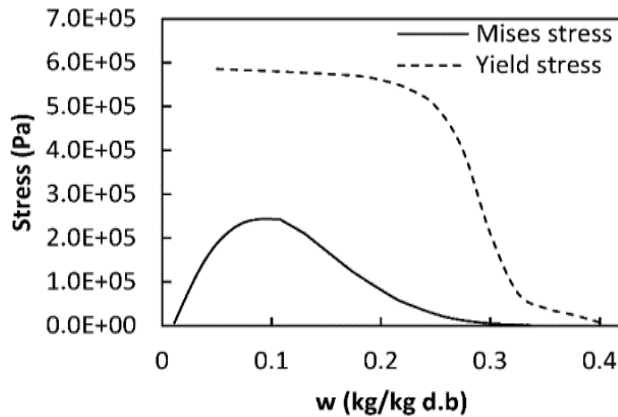


Fig. 19 comparison between maximum mises stress induced by drying and yield stress



Fig. 20 Von mises stress evolution induced by temperature changes

11. References

- [1] K. Chua, A. Mujumdar, M. Hawlader, S. Chou, J. Ho, Convective drying of agricultural products. Effect of continuous and stepwise change in drying air temperature, *Drying Technology*, Vol. 19, No. 8, pp. 1949-1960, 2001.
- [2] G. Musielak, D. Mierzwa, Permanent strains in clay-like material during drying, *Drying Technology*, Vol. 27, No. 7-8, pp. 894-902, 2009.
- [3] K. Khalili, S. y. Ahmadi-Brooghani, M. Bagherian, Experimental and numerical study of the ceramic drying process and cracking, *Journal of Solid and Fluid Mechanics*, Vol. 4, pp. 119-129, 2014.
- [4] M. Heydari, K. Khalili, Investigation on the Effect of Young's Modulus Variation on Drying-Induced Stresses, *Transport in Porous Media*, Vol. 112, No. 2, pp. 519-540, 2016.
- [5] S. J. Kowalski, 2003, *Thermomechanics of drying processes*, Springer Berlin Heidelberg,
- [6] M. Vasić, Ž. Grbavčić, Z. Radojević, Determination of the moisture diffusivity coefficient and mathematical modeling of drying, *Chemical Engineering and Processing: Process Intensification*, Vol. 76, pp. 33-44, 2014.
- [7] S. Chemkhi, F. Zagrouba, A. Bellagi, Mathematical model for drying of highly shrinkable media, *Drying Technology*, Vol. 22, No. 5, pp. 1023-1039, 2004.
- [8] W. P. da Silva, C. M. D. P. da Silva, L. D. da Silva, V. S. de Oliveira Farias, Drying of clay slabs: experimental determination and prediction by two-dimensional diffusion models, *Ceramics International*, Vol. 39, No. 7, pp. 7911-7919, 2013.
- [9] M. R. Islam, A. Mujumdar, Role of product shrinkage in drying rate predictions using a liquid diffusion model, *International communications in heat and mass transfer*, Vol. 30, No. 3, pp. 391-400, 2003.
- [10] J. Esfahani, H. Majdi, E. Barati, Analytical two-dimensional analysis of the transport phenomena

- occurring during convective drying: apple slices, *Journal of Food Engineering*, Vol. 123, pp. 87-93, 2014.
- [11] D. Mihoubi, A. Bellagi, Stress generated during drying of saturated porous media, *Transport in porous media*, Vol. 80, No. 3, pp. 519-536, 2009.
- [12] H. F. Oztop, E. K. Akpınar, Numerical and experimental analysis of moisture transfer for convective drying of some products, *International Communications in Heat and Mass Transfer*, Vol. 35, No. 2, pp. 169-177, 2008.
- [13] R. Lewis, M. Strada, G. Comini, Drying-induced stresses in porous bodies, *International Journal for Numerical Methods in Engineering*, Vol. 11, No. 7, pp. 1175-1184, 1977.
- [14] S. Chemkhi, W. Jomaa, F. Zagrouba, Application of a coupled thermo-hydro-mechanical model to simulate the drying of nonsaturated porous media, *Drying technology*, Vol. 27, No. 7-8, pp. 842-850, 2009.
- [15] K. Khalfaoui, S. Chemkhi, F. Zagrouba, Modeling and stress analysis during drying of a deformable and saturated porous medium, *Drying technology*, Vol. 31, No. 10, pp. 1124-1137, 2013.
- [16] F. Couture, S. Laurent, M. A. Roques, Drying of two-phase media: Simulation with liquid pressure as driven force, *AIChE journal*, Vol. 53, No. 7, pp. 1703-1717, 2007.
- [17] F. Augier, W. Coumans, A. Hugget, E. Kaasschieter, On the risk of cracking in clay drying, *Chemical Engineering Journal*, Vol. 86, No. 1, pp. 133-138, 2002.
- [18] K. Khalili, M. Heydari, Studying the effect of part thickness on cracking during drying process, *Modares Mechanical Engineering*, Vol. 12, No. 3, pp. 103-116, 2012.
- [19] M. Ganjiani, A damage model incorporating dynamic plastic yield surface, *Journal of Computational Applied Mechanics*, Vol. 47, No. 1, pp. 11-24, 2016.
- [20] F. Pourcel, W. Jomaa, J.-R. Puiggali, L. Rouleau, Criterion for crack initiation during drying: Alumina porous ceramic strength improvement, *Powder Technology*, Vol. 172, No. 2, pp. 120-127, 2007.
- [21] A. A. J. Ketelaars, *Drying deformable media: Kinetics, shrinkage and stresses (Ph. D. Thesis)*, Thesis, University of Eindhoven 1993.
- [22] S. Kowalski, G. Musielak, J. Banaszak, Experimental validation of the heat and mass transfer model for convective drying, *Drying Technology*, Vol. 25, No. 1, pp. 107-121, 2007.
- [23] M. Van Belleghem, M. Steeman, H. Janssen, A. Janssens, M. De Paepe, Validation of a coupled heat, vapour and liquid moisture transport model for porous materials implemented in CFD, *Building and Environment*, Vol. 81, pp. 340-353, 2014.
- [24] S. Chemkhi, F. Zagrouba, Water diffusion coefficient in clay material from drying data, *Desalination*, Vol. 185, No. 1-3, pp. 491-498, 2005.
- [25] B. A. Manel, D. Mihoubi, S. Jalila, B. Ahmed, Strain-stress formation during stationary and intermittent drying of deformable media, *Drying technology*, Vol. 32, No. 10, pp. 1245-1255, 2014.
- [26] M. Heydari, K. Khalili, Modeling Enhancement and Simulation of Distortion in Drying Process, *Modares Mechanical Engineering*, Vol. 15, No. 10, pp. 291-301, 2015.
- [27] S. J. Kowalski, A. Rybicki, Rate of Drying and Stresses in the First Period of Drying, *Drying Technology*, Vol. 18, No. 3, pp. 583-600, 2000.
- [28] G. Musielak, Influence of the drying medium parameters on drying induced stresses, *Drying Technology*, Vol. 18, No. 3, pp. 561-581, 2000.
- [29] S. J. Kowalski, J. Banaszak, A. Rybicki, Plasticity in materials exposed to drying, *Chemical Engineering Science*, Vol. 65, No. 18, pp. 5105-5116, 2010.
- [30] G. Caceres, D. Bruneau, W. Jomaa, Two-phase shrinking porous media drying: a modeling approach including liquid pressure gradients effects, *Drying Technology*, Vol. 25, No. 12, pp. 1927-1934, 2007.
- [31] K. Khalili, M. Heydari, M. Khalili, Drying Clay Bricks with Variable Young's Modulus, *Procedia Technology*, Vol. 12, pp. 382-387, 2014.
- [32] S. J. Kowalski, A. Rybicki, *The vapour-liquid interface and stresses in dried bodies*, in: *Drying of Porous Materials*, Eds., pp. 43-58: Springer, 2006.
- [33] K. Khalili, M. Heydari, Numerical modeling of shrinkage of a ceramic material in drying process, *Modares Mechanical Engineering*, Vol. 12, No. 2, pp. 58-71, 2012.
- [34] I. Hammouda, D. Mihoubi, Modelling of drying induced stress of clay: elastic and viscoelastic behaviours, *Mechanics of Time-Dependent Materials*, Vol. 18, No. 1, pp. 97-111, 2014.
- [35] J. Banaszak, S. J. Kowalski, Drying induced stresses estimated on the base of elastic and viscoelastic models, *Chemical Engineering Journal*, Vol. 86, No. 1, pp. 139-143, 2002.
- [36] D. Mihoubi, A. Bellagi, Modeling of heat and moisture transfers with stress-strain formation during convective air drying of deformable media, *Heat and Mass Transfer*, pp. 1-9, 2012.
- [37] D. Mihoubi, A. Bellagi, Two-dimensional heat and mass transfer during drying of deformable media, *Applied Mathematical Modelling*, Vol. 32, No. 3, pp. 303-314, 2008.
- [38] S. Kowalski, A. Pawłowski, Modeling of kinetics in stationary and intermittent drying, *Drying Technology*, Vol. 28, No. 8, pp. 1023-1031, 2010.
- [39] K. Behrouzi, S. F. Chini, Evaluation of Evaporation Estimation Methods: a Case Study of Karaj Dam Lake, *Journal of Computational Applied Mechanics*, Vol. 48, No. 1, pp. 137-150, 2017.

- [40] W. P. da Silva, L. D. da Silva, V. S. de Oliveira Farias, C. M. D. P. da Silva, Water migration in clay slabs during drying: A three-dimensional numerical approach, *Ceramics International*, Vol. 39, No. 4, pp. 4017-4030, 2013.
- [41] I. Hammouda, K. Jlassi, D. Mihoubi, Changes in the physicochemical characteristics of a ceramic paste during drying, *Comptes Rendus Mécanique*, Vol. 343, No. 7, pp. 419-428, 2015.
- [42] N. Shokri, D. Or, What determines drying rates at the onset of diffusion controlled stage-2 evaporation from porous media?, *Water Resources Research*, Vol. 47, No. 9, 2011.
- [43] N. Shokri, P. Lehmann, D. Or, Critical evaluation of enhancement factors for vapor transport through unsaturated porous media, *Water resources research*, Vol. 45, No. 10, 2009.